In Light and In Darkness, In Motion and In Stillness: A Reliable and Adaptive Receiver for the Internet of Lights

Qing Wang, *Member, IEEE,* Domenico Giustiniano, *Senior Member, IEEE,* and Marco Zuniga, *Member, IEEE*

***Abstract*—LEDs in our buildings, vehicles and consumer products are rapidly gaining visible light communication capabilities. LED links however are notorious for being unreliable: shadowing, blockage, mobility, external light, all of these issues can disrupt the connectivity easily. Therefore, unless a reliable and *cost-efficient* data link layer is designed, VLC will be confined to niche applications. In this paper, we reveal a reason for unreliable VLC: a single type of photodetector at the receiver can not establish a reliable link. We show that photodetectors with complementary properties, in terms of optical spectral response and field-of-view, are necessary to handle the wide dynamic range of optical noise (such as the sun and other unwanted light sources) and mobility of users. Motivated by our experimental observations, we design REAL-VLC (a reliable and adaptive receiver for VLC) for low-end communication systems, an *inexpensive* receiver that senses light with complementary photodetectors and configures itself (Physical and Data Link Layers) dynamically to maintain the communication link. We implement the hardware and the software of REAL-VLC in low-end platforms, and experimentally validate it in representative test scenarios and a proof-of-concept application that consists of mobile nodes maintaining a VLC link under various lighting and path conditions.**

***Index Terms*—Internet of Lights, Reliable link, FOV, Spectral response, Tradeoff, Design, Implementation, Evaluation**

I. Introduction

Wireless communication based on the radio-frequency spectrum has revolutionized how our societies work. After decades of research, the radio link is so-well understood that we can now embed tiny wireless transceivers in any *thing*. These great advances are enabling us to build the Internet of Things (IoT).

Exploiting the visible light spectrum could provide equally disruptive effects. Thanks to the advancements in Visible Light Communications (VLC), LED lights can now be modulated at speeds comparable to radio-frequency technologies, making them alternatives for wireless communication. Due to the high energy efficiency of LEDs, *all* light emitting devices are rapidly becoming LED-based: car/city lights, billboards, home appliances, toys, just to name a few. In the near future, *we will have a new type of pervasive infrastructure to be networked, an Internet of Lights (IoL)*. IoL will integrate communication, sensors and light, and create new pervasive smart environments for connected devices and objects, all centered around light as a communication medium.

Manuscript received February 22, 2017; revised July 15, 2017; accepted September 16, 2017. This work was funded in part by the Madrid Regional Government through the TIGRE5-CM program (S2013/ICE-2919). *(Corresponding author: Qing Wang.)*

Q. Wang is with the Delft University of Technology (Delft, the Netherlands) and the KU Leuven (3001 Leuven, Belgium). Part of the work was performed when he was a PhD student in IMDEA Networks Institute, Madrid, Spain. E-mail: *qing.wang@imdea.org*

D. Giustiniano is with IMDEA Networks Institute, 28918, Madrid, Spain. E-mail: *domenico.giustiniano@imdea.org*

M. Zuniga is with the Delft University of Technology, 2628 CD, Delft, the Netherlands. E-mail: *m.a.zunigazamalloa@tudelft.nl*

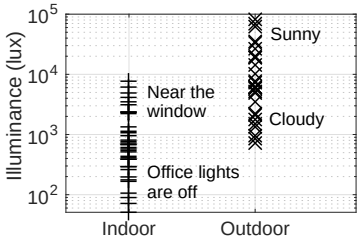

Fig. 1. The challenge for a reliable visible light communication: variation of illumination levels in various light conditions and scenarios

Achieving the vision of an IoL requires analyzing the complexity of visible light links from a *networking* perspective, and adapting to the unique properties of visible light signals (compared to radio). A first necessary step towards a new network stack is to have a reliable visible light link. However, designing such a link and embedding it into tiny wireless transceivers is a difficult task mainly due to two challenges:

Challenge 1: Exposure to high variations of illuminance level. Visible light signals are exposed to abrupt changes in noise floor. We measure experimentally the illuminance in representative scenarios and report the received Lux in Fig. 1. A drastic variation in illuminance can occur for a receiver moved from an indoor space with lights off (≈ 100 lux) to outdoor areas with sunlight (10^5 lux), causing an increase of 30 dB in the noise floor. These changes can saturate optical receivers, making VLC links disappear. The problem is exacerbated by the fact that we can not control the interference sources. The visible light spectrum is unlicensed, with the sun as a major source of communication interference to VLC. Artificial lights will also continue to be deployed and used mainly to serve the purpose of illumination. The IoL will need to make the best out of the artificial lights by piggybacking information on them without dictating how lights are to be used.

Challenge 2: Unstable links in mobile scenarios. The directionality of LED lights is determined by illumination needs. For communication purposes, directional sources are good for avoiding collisions and spectrum reuse, but undesired for discovering and maintaining links in mobile settings [1]. While piezoelectric devices could be used to steer a light beam towards the desired receiver in mobile settings, beam steering would disturb the illumination provided to the user. The problem of uncontrollable directivity is exacerbated by the receiver. Photodetectors are only sensitive to the light received within its given Field-of-View (FOV). The mobile link can be

easily broken when the light emitted from the transmitter is out of the receiver's FOV.

Our contributions. To tackle these challenges, in this work we exploit the unique characteristics of different photodetectors – photodiodes and LEDs (can operate as photodetectors) – each photodetector has different properties in terms of the saturation level, directionality, and coverage. We propose a novel cost-efficient receiver – *REAL-VLC (reliable and adaptive receiver for VLC)* – to increase the reliability of visible light links by combining photodetectors with complementary properties. We summarize our main contributions as follows.

1) We identify the need for a multi-photodetector receiver and provide a *deep analysis* on the necessary design tradeoffs. We show that LEDs (acting as receivers) and photodiodes have complementary properties in terms of transmission range, saturation point and directionality. This insight allows us to design a receiver that is robust to mobility and various illumination levels, from complete darkness to daylight (Sections III–IV).

2) We design, implement, and evaluate a platform and network stack, from the Physical to Data Link Layers, for sensing and receiving data according to the surrounding illuminance level. The receiver is able to switch seamlessly among different receiver configurations within the same frame (Section V).

3) We showcase the applicability of our findings on a scaled down application, where two mobile nodes try to maintain a link under different types of paths, straight and curves, and different illumination conditions, day and night. Our results show that our receiver is able to maintain a constant link while a classical receiver can only offer intermittent connectivity (Section VI).

II. Background and Objectives

A. The optical efficiency of VLC links

In VLC, LEDs are modulated to transmit information. This modulated light impinges upon the receiver and is transformed into current. The *spectral response* of the receiver determines how much light is transformed to current. The current changes are then decoded into information. A key parameter to determine the efficiency of VLC links is the coupling of the spectral responses of the transmitter and receiver. Let us denote $S_{\mathrm{TX}}(\lambda)$ and $S_{\mathrm{RX}}(\lambda)$ as the normalized spectral response of the transmitter and receiver, respectively. The optical efficiency of VLC links can be formulated as [2], [3]:

$$\gamma = \int_0^\infty S_{\mathrm{TX}}(\lambda) S_{\mathrm{RX}}(\lambda) d\lambda \tag{1}$$

The maximum efficiency is achieved when the above two spectral responses match well, i.e., their shapes should be similar and fall into the same range of frequency. The importance of this matching effect is depicted in Fig. 2 and explained below:

- *Wasted signal energy:* part of the luminous power emitted by the transmitter is not captured by the receiver, leading to wasted signal-energy and a shorter communication range.
- *Unnecessary noise:* the receiver absorbs all the luminous power of the transmitter, but also is exposed to the spectrum that brings unnecessary noise that degrades the link quality.

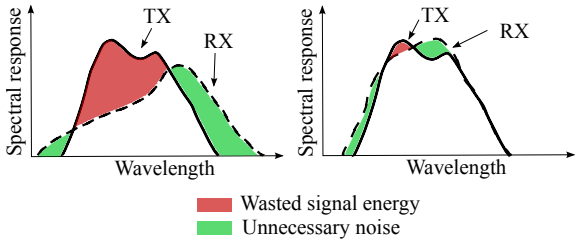

Fig. 2. VLC spectrum - example of inefficiency in the optical communication

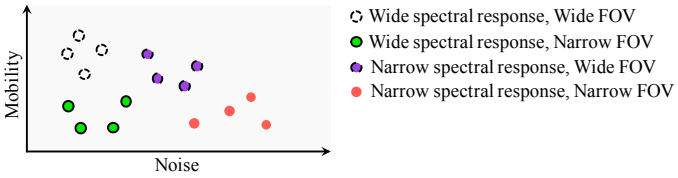

Fig. 3. Trade-offs of the receiver spectral response S_{RX} and the FOV

B. Trade-offs of spectral response and FOV

A good coupling of the spectral responses can increase the performance of the link. However, it is difficult to achieve in many scenarios. First, devices have no control over the spectral response S_{TX} of interfering light sources (Challenge 1). VLC links absorb a large amount of illuminance power from light sources containing either no information (sunlight) or undesirable information (other transmitters). Second, the concept of optical efficiency does not include the limitations posed by the FOV of photodetectors. In mobile scenarios, link disruption could be frequent and pervasive (Challenge 2).

Possible solutions to the challenges are intertwined, causing a trade-off that we have to address. Since we cannot change the spectral response S_{TX} or direction of visible light transmitters (illuminance is the primary application of LEDs), we can only act on the receiver to overcome the aforementioned problem in two dimensions: *change the FOV and/or the spectral response of the receiver.*

Fig. 3 illustrates the overall tradeoffs posed by the receiver's spectral response and FOV. The first approach is to adopt a narrow FOV at the receiver, capable of pointing only to the direction of desired light source ("narrow FOV" in Fig. 3). While this would increase the resilience of VLC links to external noise sources (addressing Challenge 1), it would become more vulnerable to mobility (Challenge 2 is not addressed). The second approach is to reduce the sensitivity of the receiver in part of the spectrum response S_{RX} ("narrow spectral response" in Fig. 3). While this would reduce the amount of illuminance received from external light sources, necessary to avoid the saturation of the optical receiver, it would also reduce the communication range in many scenarios.

C. Objectives of this work

Considering the above presented tradeoff, our design goals in this work are as follows:

- Goal 1: *design an optical front-end that can provide a reliable communication under light, darkness, mobile, and static settings using unmodified white LEDs as transmitters.*
- Goal 2: *design a system that is simple, cost-efficient, and energy-efficient so a wide community could benefit from it.*

To the best of our knowledge, we are the first to investigate this tradeoff targeting at designing a resilient and cost-efficient platform, and to propose and evaluate a potential solution.

III. Basic Design: Sensing Light with Two Complementary Photodetectors

A perfect optical receiver would be one that can adjust its spectral response and FOV dynamically according to the scenario at hand. That would be a very complex and costly optical Micro-ElectroMechanical Systems (MEMS) to build, thus failing to meet Goal 2 in Section II-B. What is available is a broad array of inexpensive and commodity optical receivers, with various spectral responses and FOVs, to suit the requirements of specific scenarios. Based on this availability, we consider two types of commodity optical photodetectors: i) photodiodes (PDs); and ii) LEDs used for reception (RX-LED). We show that each of them has unique and complementary features.

Wide spectral response and wide FOV. As shown in Fig. 3 (white dots), photodetectors of this type can be used on scenarios with low noise and high mobility. Commodity PDs are well suited for these applications. They have a wide spectral response (often including the infrared spectrum) and a wide FOV, with a half angle, e.g. angle of half intensity, of up to 60^o–75^o. The wide spectral response increases the range, and the FOV provides a reasonable trade-off between being narrow enough to avoid interference but also wide enough to make the link relatively stable to mobility.

Narrow spectral response and narrow FOV. The most prominent source of noise is sunlight, which is wideband and may greatly deteriorate the communication link, because it emits energy over the entire spectral response of the PD. We exploit two factors to address this problem:

- The spectral response S_{TX} of the LED transmitters is not uniform in the visible spectrum. There are two peaks: one around the blue color and another one dependent on the type of white: cool white, natural white, and warm white [3].
- There is a family of low-cost and commodity RX-LEDs (5 mm LEDs operated in reverse bias) with narrow spectral response and narrow FOV [4], [5] (red dots in Fig. 3).

Based on these, we use a RX-LED such that its peak is close to one of the two transmission peaks of the white LED. An illustration is given in Fig. 4. This allows us to efficiently reject all noise components outside its narrow spectrum response (in particular the sun). The narrow FOV also helps with discarding unintended light sources from different directions.

A. Selected complementary photodetectors

Next we describe the selected optical devices. The photodetectors (PD and RX-LED) and optical emitter (White LED) we use in the experiments are shown in Fig. 5.

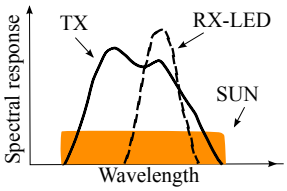

Fig. 4. RX-LED used as photodetector. Its narrow spectral response filters a large compoment of the noise from the sun and reduces the risk of saturation.

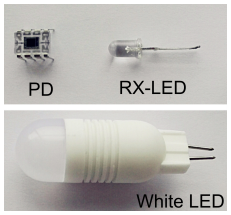

Fig. 5. Optical elements in our proposed system

White LED. For transmission, we use a white LED bulb. The small bulb is chosen to resemble the coverage characteristics of most LED luminaries: white light with a view angle of 160^o. The warm color of the white LED we use corresponds to 3000^o Kelvin and has two peaks in the spectrum, in the blue color at 450 nm and in the red color at 600 nm [3].

Photodiode (PD). The first commodity photodetector in our platform is a widely popular PD used for sensing applications with VLC [6]. This PD has a wide spectrum response in the visible spectrum and part of infrared spectrum (spectral halfwidth of 450 nm) and a wide coverage (the FOV is 75^o).

Receiver LED (RX-LED). To complement the PD, the second commodity photodetector must have narrow spectral response and narrow FOV. Commodity PDs with narrow spectral response are still in their research stage, and currently they can be built only combined with optical filters [7]. This increases their overall cost and architectural complexity (thus they do not fulfill Goal 2 in Section II-B). Instead, we use commodity LEDs as photodetectors. Next, we explain the reasoning for selecting the LED as a receiver.

1) Analysis of the spectral response of RX-LED: We use an LED that according to the specification has a peak at 626 nm when operated as transmitter (forward bias) and a narrow band spectrum response (spectral halfwidth of 17 nm), which results in the emission of red color. We do not use the LED as transmitter though, but rather as receiver (reverse bias). Since the default operation of LEDs is not to act as photodetectors, a datasheet for reception performance is missing. Therefore, we have to infer the spectral response of the LED acting as receiver (RX-LED). It has been demonstrated that the peak detection of RX-LEDs is shifted by a few short wavelengths when operated as receivers with respect to their operation as transmitters, and the bandwidth is slightly larger than the corresponding spectrum response as transmitter [8]. For our RX-LED, this corresponds to a peak detection that is very close to the peak of 600 nm of the warm white LED we use as transmitter. In addition, the spectral halfwidth as receiver is approximately 80 nm (narrow spectrum response), more than five times smaller than the PD's spectrum.[1]

B. Advantages and limitations

We empirically evaluate the sensing capabilities of PD and RX-LEDs and characterize their advantages and limitations.

[1]This calculation assumes that our LED is similar the one used in Fig. 1 in [9]. The authors evaluate an LED that has the same spectrum response as our LED when operated as transmitter (forward bias), unfortunately the authors do not specify the LED model, thus we cannot confirm our hypothesis.

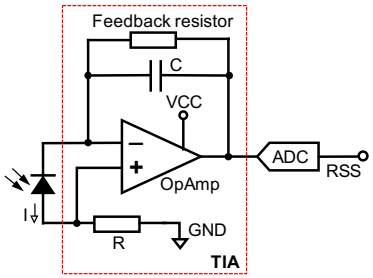

Fig. 6. The schematic of the receiver

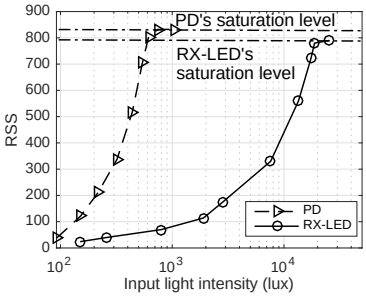

Fig. 7. Measurements of the ambient noise under different scenarios. *The RSS is the number read from the ADC. The DC gain of the PD is* 1×10^6. *The power supply is +5V. The saturation depends on the specific optical device. In this figure, the saturation points are of the PD and the RX-LED, therefore, the RSSs of the saturation points are different.*

Limitation of PDs: saturation. We first evaluate the fundamental limits of a PD receiver. To achieve this, we measure the illuminance using the PD and the RX-LEDs under different light conditions: indoors with office lights off and on, moving an additional lamp gradually close to node A, and outdoors during the day at various light conditions. A high-level schematic of the receiver circuitry is shown in Fig. 6. The illuminance under each condition is measured by the receiver and a commercial light meter. The results are given in Fig. 7, where the y-axis denotes the estimated Received Signal Strength (RSS) as a function of the illuminance measured by the light meter. The RSS is measured at the receiver's Analog-to-Digital Converter (ADC).

We observe from Fig. 7 that the PD is very sensitive to light changes. When the ambient light intensity is above $750\,\text{lux}$, the PD reaches its saturation state, because of the wide spectral response S_{RX} that indiscriminately absorbs visible light (and often infrared frequencies). As a reference, $500\,\text{lux}$ is the illuminance level that is normally observed in office areas, cf. Fig. 1. The RX-LED is instead less sensitive at this level of illuminance. This is due to the narrow FOV of RX-LEDs (acting as a spatial filter and allowing the RX-LED to absorb energy coming only from a small angle) and the inherent narrow S_{RX} that rejects by default a large part of the optical spectrum. The RX-LED remains clearly unsaturated for values below $10000\,\text{lux}$, which map to full daylight (cf. Fig. 1). Therefore, the PD alone is not resilient enough to provide a reliable VLC link (since it is easily saturated at all times outdoors and sometimes indoors), instead the RX-LED only gets saturated when exposed to full daylight.

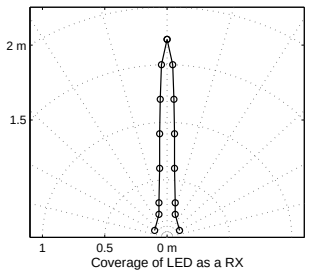

Fig. 8. Coverage of a RX-LED

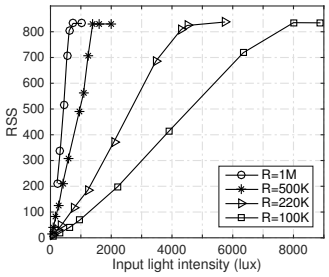

Fig. 9. Measured RSS using a PD and different feedback resistors R

Limitation of RX-LEDs: directionality. As experimentally shown in the previous test, RX-LEDs are good at filtering optical noise for scenarios with high illuminance. Their main limitation however is their strong directionality. This causes RX-LEDs to be more susceptible to link instability due to mobility. To depict this problem we perform the following experiment. We fix the position of platform A (transmitter with the white LED) and move platform B (receiver with RX-LED) around different locations within a sector of $2\,\text{m}$, as shown in Fig. 8. We can observe that the reception range of the RX-LED is narrow in space, around $15\,\text{cm} \times 200\,\text{cm}$. This would make RX-LED links intermittent under mobility.

Concluding, *a joint PD-LED receiver can potentially be a low-cost alternative to expensive MEMSs to provide reliable links, thanks to complementary features of PDs and RX-LEDs*.

IV. Tradeoff Analysis of Our Photodetectors

We now quantify the tradeoffs in terms of communication range, resilience to external illumination and directionality of fundamental design in Sec. III. This analysis will allow us to present the system design of our REAL-VLC.

A. Gain control

In order to avoid saturation for reasonable background illumination, we have to configure the receiver to select the most appropriate gain level. While we cannot reconfigure the optical package, sensing area and other optical parts once the photodetector has been selected, we instead can control the feedback resistor R used in its amplifier circuitry (cf. Fig. 6).

To analyze the tradeoff related to controlling the feedback resistor, we consider two facts. First, the photodetector produces a current I that is directly proportional to the received instantaneous power [10]. Second, we can express the RSS as $\text{RSS} = k_1 \cdot R \cdot I$, where k_1 is a constant factor and I is the current generated by the impinging light into the photodetector [11][2]. From these two facts, it follows that:

$$\text{Sensitivity} = \delta\text{RSS}/\delta I = k_1 \cdot R, \tag{2a}$$

$$\text{Saturation} = k_2/\text{R}, \tag{2b}$$

where the Saturation is computed for maxRSS (maximum RSS can be reached) and $k_2 = \text{maxRSS}/k_1$. The trends

[2]This holds for a photodetector with an Operational Amplifier (OpAmp) used as TransImpedance Amplifier (TIA) (cf. Fig. 6)

captured by these equations can be observed in Fig. 9, where we measure the RSS values in our platform under different illuminance conditions and with different resistors R. Reducing R from $1\,\mathrm{M}\Omega$ to $100\,\mathrm{K}\Omega$ increases the resilience to saturation (from $750\,\mathrm{lux}$ to $\approx 7\mathrm{K}\,\mathrm{lux}$), but the values are still well below the illuminance conditions observed on cloudy days ($10\mathrm{K}\,\mathrm{lux}$).

From Eq. (2a) and Eq. (2b) and the experiments above, we can derive the following trade-off:

- A large R implies that small changes in current (i.e. small variations in the amount of impinging light) give noticeable changes in RSS. This leads to a very high sensitivity, ideal for long reception ranges in dark scenarios.
- A small R has the opposite effect, more impinging light is required to differentiate '1' and '0' bits (less sensitivity), but the photodetector is more resilient to external light sources.

Fig. 11 shows the tradeoff between the coverage range and resilience to illuminance. We observe a Pareto frontier curve for the PD. Note that fine-tuning the resistor R is a loosing proposition because tradeoffs lead to an inward (convex) curve towards the worst case point [0,0], instead of an outward (concave) curve towards a better operational point [longer range, more resilience]. For the RX-LED, we use a fixed value $R = 1\,\mathrm{M}\Omega$ due to two reasons/observations:

- the RX-LED's saturation point is high enough ($>10\,\mathrm{K}$ lux) when $R = 1\,\mathrm{M}\Omega$. Therefore, we do not need to reduce R to increase the saturation point further;
- we designed the RX-LED and PD to provide the same data rate; increasing R would reduce the RX-LED's data rate (a higher R can further distort the received signals).

Quantification of the angular coverage. The coverage analysis has so far implicitly considered that the transmitter is placed perpendicular to the surface of the photodetector. We now place the receiving platform B at position [0,0] and the transmitter platform A is placed over various concentric circles around [0,0]. At each location, platform A sends packets using the white LED. The results are shown in Fig. 10. We observe that reducing the value of the resistor R leads to a significant reduction of the angular coverage, in particular on settings with relative low illumination. In addition, from Fig. 10(d), we observe that the communication range of the PD collapses before reaching the saturation level: $500\,\mathrm{lux}$ vs. the 750 lux requires for saturation. This is due to the fact that, given the output power of the LED transmitter and the surrounding light (noise floor), the SNR is too low to decode information. Overall, our results lead to the following insight.

Insight 1: The VLC link only benefits partially from reducing the resistor R to increase resilience of PDs to higher levels of illumination. This is because the reception coverages decrease significantly with smaller R. As such, the fundamental problem of link saturation can not be solved solely by adjusting the configuration of the feedback resistor R. In addition, we should use a RX-LED with a fixed R.

B. Operational regions

We compare the angular coverage of RX-LED and PD for various illumination levels and show the results in Fig. 10. We can identify three main operational areas. First, in dark scenarios, Fig. 10(a), the RX-LED adds nothing to the link's performance: its coverage is a small subset of the PD's. Second, under mild illumination conditions, Fig. 10(b)-(c), the RX-LED adds some benefit. Third, in normal indoor lighting conditions, Fig. 10(d), the RX-LED is the only alternative. Note that the coverage of the RX-LED does not change under different illumination conditions. This property is the main advantage of RX-LEDs. Overall, the experiments performed with the RX-LED as a receiver lead to the following insight:

Insight 2: A RX-LED provides a constant but narrow reception coverage across various illumination conditions. Given the much larger coverage of PDs under darker conditions, RX-LEDs should be used for reception only under medium and high illuminance conditions.

V. System Design: REAL-VLC

We introduce REAL-VLC, a REliable and Adaptive Link for VLC. Ideally we would like a system that works under all lighting conditions (from complete darkness to strong interfering light) and that maintains a wide and long coverage under all these conditions. But as shown in the previous section, there is no one-size-fits-all solution. The tradeoffs related to coverage, saturation and directionality require a multi-layer solution at HW, PHY and MAC. To provide a solution for these tradeoffs, we build a flexible receiver that can reconfigure itself sufficiently fast in the presence of drastic changes of illuminance levels and user mobility.

*The receiver has been integrated into the OpenVLC platform (www.openvlc.org) and will be made available for the research community to investigate new networking challenges arising from the IoL.*OpenVLC is an open source project that extends an embedded board to perform visible light communications. It was first presented in [12]. The Physical Layer uses On-Off-Keying modulation with Manchester coding. Data is then transmitted using intensity modulation, where binary information is mapped to the presence (symbol HIGH) or absence (symbol LOW) of the visible light carrier. The advantage of using this platform, compared to others in the community [5], [13], is that it runs Linux and it is seamlessly integrated with the TCP/IP stack. In this work, we extend OpenVLC in hardware, and software at the PHY and MAC layers. The overall design of our system is shown in Fig. 12, and a picture of the hardware and the list of the used electronic devices are given in Fig. 13. We describe our extensions and methods in the following subsections.

A. Hardware Layer: design of the receiver

The first important change we made to the original platform is to design a new front-end. The original OpenVLC platform had a single low-power LED used both for transmission and reception [12], [4]. In this work, we add a high power white LED and customized driver circuit for transmission. For reception, we add a PD and its ancillary circuitry. We also reuse the original circuitry to amplify the signal of the low-power LED and operate it *solely* as RX-LED.

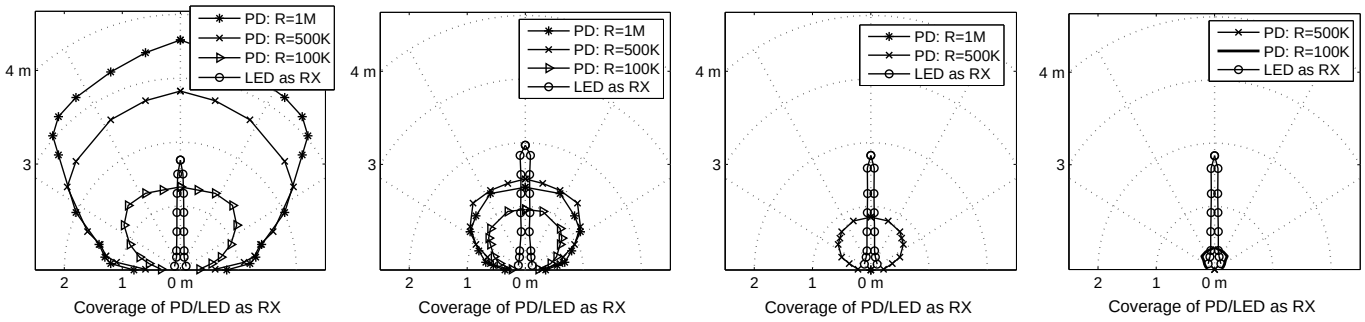

(a) Noise floor = 10 lux (b) Noise floor = 220 lux (c) Noise floor = 350 lux (d) Noise floor = 500 lux

Fig. 10. Angular coverage of PD and RX-LED for various illumination levels

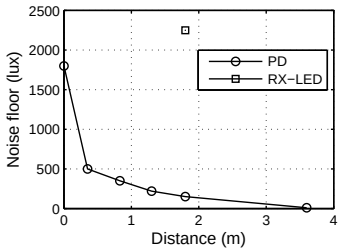

Fig. 11. Pareto frontier of PDs and RX-LED point (the measured results depend on many factors, such as the type of PD and the power supply of the amplifier. In this measurement, the used PD is the OPT101; the power supply of the amplifier is +5V)

B. Physical Layer: adaptation to surrounding illuminance

From the analysis in Section IV, it follows that a receiver should sense the surrounding light intensity and adjust itself to the best corresponding configuration to decode noisy data. To allow a fast reconfiguration process, we constantly monitor and adapt two parameters: gain control and decoding threshold.

Dynamic gain control. The aim of this parameter is to reduce the exposure of the PD to saturation levels by adjusting its sensitivity, and thus, allowing the correct decoding of frames. To achieve this aim, we use a set of carefully-selected feedback resistors R and develop a software-defined controller to change the resistor on-the-fly based on the estimated SNR.

Since the noise level can change abruptly during a frame transmission, we have to dynamically measure the SNR *within* the frame. Therefore, we cannot use information about the noise level before frame reception. To solve this problem, we use the RSS values measured at the ADC output (cf. Fig. 6) and estimate the SNR without measuring the noise floor, as proposed in [14]:

$$\mathrm{SNR}_{\mathrm{M2M4}} = \frac{\frac{1}{2}\sqrt{6M_2^2 - 2M_4}}{M_2 - \frac{1}{2}\sqrt{6M_2^2 - 2M_4}}, \tag{3}$$

where M_2 and M_4 indicate the second and fourth moments of the RSS, respectively. The adaptation of the PD's gain control based on $\mathrm{SNR}_{\mathrm{M2M4}}$ is provided in Algorithm 1.

Adaptive decoding threshold. After changing the sensitivity of the PD, the receiver needs to update the decoding threshold. To convert symbols into binary data, an *adaptive* threshold is adopted to distinguish between HIGH and LOW symbols in the visible light carrier (direct detection). This adaptive approach is necessary to deal with drastic in-frame variations of signal strength and noise floor level. This threshold must also consider that, depending on the symbol rate, implemented electronics and budget cost of the low-end receiver, LOW symbols may not go down all the way to the level of the noise floor before frame reception. This occurs because the internal capacitor may not discharge fully at the selected transmission rate. The detection threshold is first obtained on a per-frame basis by averaging out the digital samples of the preamble sequence. During the reception of a frame, the threshold will be reconfigured, especially if the sensitivity level has been changed. The new threshold value is recalculated by averaging out a pre-fixed set of the latest received samples.

[3]If a certain amount of the raw RSS values in the stream `symStream` reach `maxRSS`, then the PD is declared to be saturated.

Algorithm 1 The PD's sensitivity adaptation.

Input: `symStream`: symbol stream (RSS values); `sensLevel`: current sensitivity level; `minSensLevel` / `maxSensLevel`: min / max supported sensitivity level; `minSNR`: minimal required SNR to decode a frame
Output: `sensLevel`: adapted sensitivity level.

```
calculate the SNR_M2M4 from symStream based on [14]
if SNR_M2M4 < minSNR then
    if PD's saturation is detected[3] then
        if sensLevel > minSensLevel then
            sensLevel ← sensLevel-1
        end if
    else
        if sensLevel < maxSensLevel then
            sensLevel ← sensLevel+1
        end if
    end if
end if
return sensLevel
```

C. Data Link Layer: parallel decoding of two photodetectors

As shown in Fig. 10, except for the very extremes of the illumination spectrum (very dark or very bright), many intermediate scenarios will require both receivers to be active. We make full use of the two photodetectors provided at the PHY layer by adopting two potential implementations for the receiver, illustrated in Fig. 14.

Additive decoding. In Fig. 14(a), the PD and RX-LED sum up their received signals after the ADC, symbol by symbol. Then we perform the framing and error handling. The

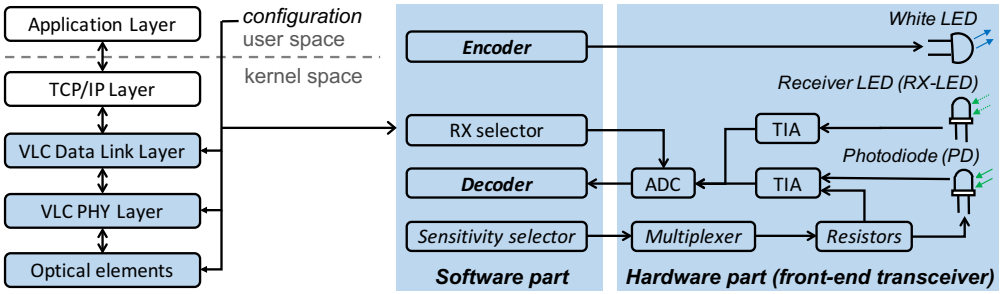

Fig. 12. System architecture: *left)* communication stack; *right)* block diagram of the front-end transceiver.

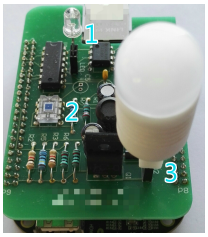

Model	Description
HLMP-EG08 -YZ000 (5mm, red)	RX-LED
sevenON, 2.5W	White LED
OPT101	PD
74HCT244N	8-bit tri-state buffer
LM358N	transimpedance amplifier
MCP3008	10-bit ADC
ADG444	4-channel multiplexer

Fig. 13. The prototype of our system. *(Left)* the front-end transceiver where the three optical elements are: 1) RX-LED; 2) PD; 3) White LED. *(Right)* the key electronic components used in our system.

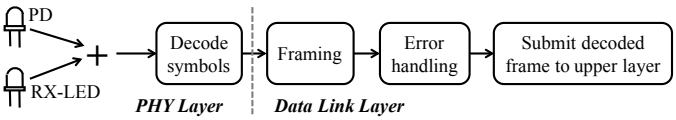

(a) Summing up the received signal of the PD and RX-LED

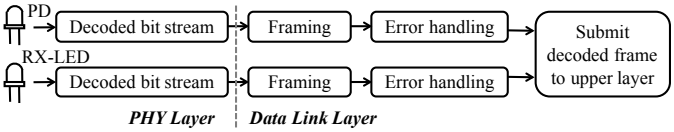

(b) Process the PD and RX-LED in parallel

Fig. 14. Process the received signals from the PD and RX-LED at the receiver

advantage of this approach is that it requires only one receiver chain (a cost effective implementation).

Parallel decoding. In Fig. 14(b), the PD and RX-LED receive light signals in parallel, with one chain per photodetector. In this implementation, the Data Link Layer requests the PHY layer to provide separated decoded signals for the PD and RX-LED. Then it performs framing and error handling per each receiver chain and only forwards a successfully decoded frame.

VI. Performance Evaluation

In this section, we evaluate the proposed adaptive receiver under increasingly complex test cases to quantify the performance of our visible light link under changes in illumination, direction and mobility. The main electronic devices adopted in our experiments are mainly listed in Fig. 13(right). We will compare the performance of different settings of the receiver as follows:

- *SoloPD-X*: only the PD is used as receiver and the sensitivity of the PD is fixed to a certain level. In the evaluation, three sensitivity levels of the PD (L1, L2, and L3) can be selected where the sensitivity levels are determined by the feedback resistor R (c.f. Fig. 6) with the value of $1M\Omega$, $220K\Omega$ and $100K\Omega$, respectively[4].
- *SoloRX-LED:* only the RX-LED is used as receiver.
- *REAL-VLC:* the receiver proposed in this work. The PD and the RX-LED are used in parallel to detect light signals. The sensitivity levels of the PD adapt to the current noise floor.

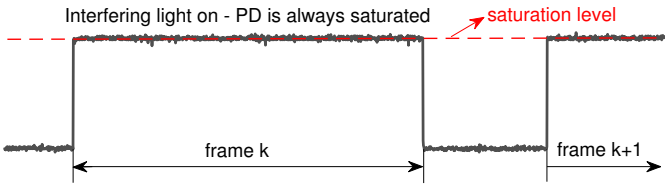

(a) Resulting RSS by summing up signals received by the PD and the RX-LED during the reception of frames (with interfering lights on)

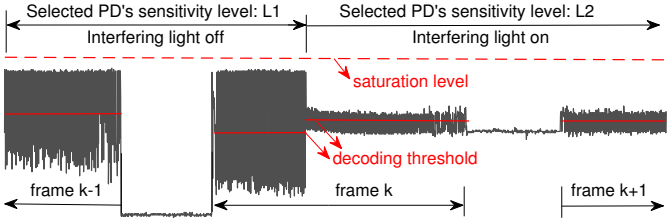

(b) Measured RSS when adapting the PD's sensitivity and the system's decoding threshold during the reception of a frame. The adaptation can be done in the symbol level, as demonstrated within the frame k

Fig. 15. Change on-the-fly re-configurations of the receiver.

A. Adaptation to sudden environment changes

We first describe how our adaptive receiver copes with sudden changes in the environment. This capability is illustrated in Fig. 15, where an oscilloscope is used to measure the voltage signal at the receiver during frame transmissions.

Fig. 15(a) highlights the benefit of using parallel decoding instead of additive decoding. In this setup, an interfering light is *on* throughout the experiment and the Data Link Layer receives information via additive decoding, c.f. Fig. 14(a). We can observe that when the frames (e.g. the frames k and $k+1$

[4]We do not use very low values of R (e.g., $10K\Omega$ or $1K\Omega$) in this section due to the fact that they can shorten the communication distance greatly.

as shown in Fig. 15(a)) are transmitted, the receiver saturates. Note that we cannot even detect the flanks going down for zero symbols. The reason is that even with the lowest PD sensitivity, the superimposition of the ambient light interference and the light emitted from the transmitter was sufficient to saturate the PD. Furthermore, we perform the same experiment but with parallel decoding. The results are shown in Fig. 15(b). We observe that the RX-LED is able to decode information, but the PD could not due to its saturation. When this already saturated signal of the PD is added to the RX-LED signal, the information from the RX-LED also gets lost. Thus, the cost of having individual decoding chains for the PD and RX-LED is worthwhile. *Since parallel decoding outperforms additive decoding, the former is selected to decode the received signals in REAL-VLC in the rest of the evaluations.*

Fig. 15(b) showcases the importance of adapting the receiver's gain control and decoding threshold. Initially the PD receives frame *k-1* in a dark scenario. Due to the dark surrounding, the receiver selects the highest sensitivity level (L1) and obtains the corresponding decoding threshold (solid red line). During the reception of the second frame k, an interfering light is turned on. The intensity of this interfering light is sufficient to saturate the receiver, but the adaptive gain control detects the change in the noise floor and reduces the sensitivity of the PD to level 2 (L2) within the frame, avoiding data losses. After adjusting the sensitivity, the adaptive threshold is adjusted as well, otherwise the signal would have been detected as a sequence of ones.

B. Bit Error Rate (BER)

We now evaluate the performance of BER under different configurations and ambient light conditions. We use two nodes, one acting as the transmitter and the other as the receiver. The transmitter keeps sending data streams to the receiver. Each data stream consists of a preamble of 24 bits and a payload of 320 Kb/s. The Physical symbol rate is set to 50K symbols/s. The two nodes are placed at a distance of 5 cm apart from each other[5]. We test the BER performance under different ambient light conditions (noise floor) where the noise floor is changed from 10 lux to 13K lux.

The evaluation results are shown in Fig. 16. First, we can observe that when the PD is not saturated[6], the BERs under the SoloPD-*X* are low and stay constant, which are around 6×10^{-6}. However, they increases fast to 100% when the PD gets close to its saturation points. Second, when the transmitter and the receiver are well aligned, the BER under the SoloRX-LED (denoted as *'SoloRX-LED (0°)'*) is more resilient to the changes in the noise floor under well-illuminated conditions (when the noise floor is higher than 4K lux), compared to the PD. Due to the narrower spectral response and narrower FOV of the RX-LED, the BER performance of the SoloRX-LED is worse than those of the PD when the PD is not saturated, or when the RX-LED is not well aligned with the transmitter

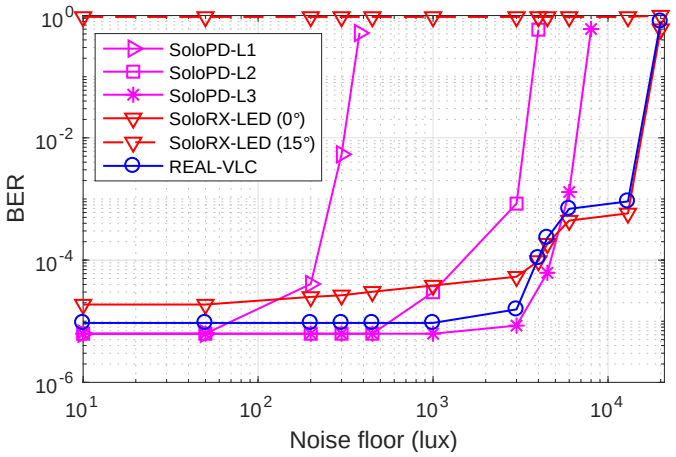

Fig. 16. The BER performance under different light conditions. *In this figure, 'SoloRX-LED (0°)' denotes the scenario where the RX-LED and the transmitter are well aligned. Similarly, 'SoloRX-LED (15°)' denotes the scenario that the RX-LED and the transmitter are misaligned by an angle of 15° (the FOV of the RX-LED is 8°).* The BER under REAL-VLC increases significantly to nearly 100% when the noise floor reaches 2×10^4 because the RX-LED has been saturated.

(dashed line denoted as *'SoloRX-LED (15°)'*). Third, the BER performance of REAL-VLC is resilient to the changes in noise floor (except when the noise floor exceeds 13K lux) and to the alignment conditions between the nodes. This demonstrates the reliability of our communication link. Due to the computation overhead[7] on decoding two parallel streams received from the PD and RX-LED, REAL-VLC's BER performance is slightly worse than those of SoloPD-*X* when the PD is far from being saturated. Similarly, REAL-VLC's BER performance is slightly worse than that of SoloRX-LED when the noise floor is high (exceeds 4K lux) and the nodes are well aligned.

C. The mild case: static nodes, no line-of-alignment

We now test the resilience of our system for maintaining a constant throughput in dynamic settings. We measure the throughput at the Application Layer. As mentioned before, the software of our system is implemented as a Linux driver connected to the TCP/IP layers. Thus we can measure the platform's throughput using the widely popular *iperf* tool. In our setup, the IP addresses of the nodes are set to 192.168.0.1 and 192.168.0.2, respectively. We run each experiment with UDP traffic for 320 seconds, and set *iperf* to report the throughput every 5 seconds. The payload of each UDP packet is set to 1000 bytes. The symbol rate at the Physical Layer is fixed to 50K symbols/s. We use the White LED (cf. Fig. 13) as the optical transmitter. The two nodes are positioned 0.5 m apart (*the distance can be easily extended to 2.5 m with a brighter and narrower-FOV LED, as will be presented in Sec. VI-D).* We change the environment in two ways: by turning on/off the light bulbs in the office and by changing the angle of view between the two nodes. We change the

[5]The BER will increase while the distance is increased, as in other wireless communications. Besides, it is important to point out that the communication distance of our system can easily reach 2.5 m, as presented later in Sec. VI-D.

[6]The saturation points of the PD with the sensitivity levels L1, L2, and L3 are around 500 lux, 4500 lux, and 8000 lux, respectively (cf. Fig. 9).

[7]In our current implementation, the sampling is performed by adopting the timer function provided by the Linux kernel. Therefore, the decoding and the sampling share the same CPU. When more CPU cycles are used by the decoding, the timer function of the Linux kernel is not accurate anymore and thus affects the BER performance.

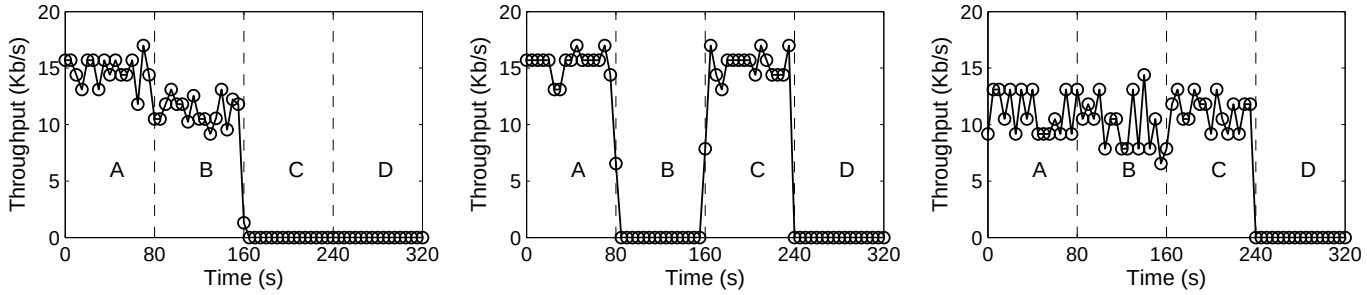

(a) SoloRX-LED: only the RX-LED is the RX

(b) SoloPD-L1: only the PD is the RX (the sensitivity level is set to L1)

(c) REAL-VLC: both the PD and the RX-LED are the RXs

Fig. 17. Evaluation results of the UDP throughput under dynamic settings

alignment between two nodes from 0^o to 45^o by hand, and the process takes roughly one second (between 160 s and 161 s). Fig. 17 shows the results under the following different setups.

Setup A: from 0 s to 80 s, angle is 0^o, lights are off.
Setup B: from 81 s to 160 s: angle is 0^o, lights are on.
Setup C: from 161 s to 240 s, angle is 45^o, lights are off.
Setup D: from 241 s to 320 s, angle is 45^o, lights are on.

Fig. 17(a), (b) and (c) show the results of using only the RX-LED as a receiver (SoloRX-LED), only the PD as a receiver (with the de-facto highest sensitivity level SoloPD-L1), and our REAL-VLC. The high directionality of RX-LED suffers for wide line-of-view angles, setups C and D in Fig. 17(a). The SoloPD-L1 on the other hand is resilient to these changes in directionality but it is exposed to saturation effects and the link disappears at high illumination conditions, setups B and D in Fig. 17(b). Our REAL-VLC maintains a reliable link in all settings except for the last one, setup D in Fig. 17(c), where the high illumination saturates the PD and the wide angle renders the RX-LED ineffective. Note that the throughput of our system is 2-3 Kb/s lower for the setups A, B, and C. This occurs due to the extra overhead incurred by monitoring the noise floor and processing the two streams of data in parallel.

D. The challenging case: mobile nodes, no line of alignment

Until now we have evaluated the resilience of our link in scenarios where nodes do not move. These type of scenarios are of interest because most lights are fixed, such as indoor light in buildings or street lighting. However, other scenarios may have mobile nodes with LED lights, for example, cars and motorbikes. In this subsection we show the performance of our link in a scaled down mobile setup.

We use two nodes as shown in Fig. 18, where node A "chases" node B. Two RX-LEDs (HLMP-EG08-YZ000) are placed street light parallel at node A to handle better mobility because the FOV of a single RX-LED is narrow. We use the White LED at node B as the light emitter. At the beginning, we place the two nodes 0.5 m apart from each other (*the distance can be easily extended to 2.5 m with a brighter and narrower-FOV LED, as stated later)*. Then we move the two nodes manually but continuously at approximately the same speed (5 cm/s). The aim is to maintain a reliable link under different types of paths, straight and curves, and under

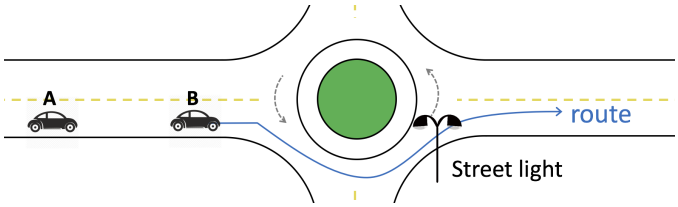

(a) Illustration

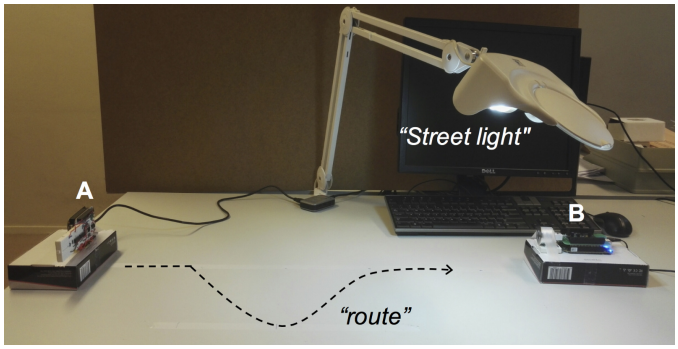

(b) Snapshot of the experimental setup

Fig. 18. Application test: route of the mobile nodes and environment setup *Two different types of LEDs are used in the experiments to support different communication distance: (i) the White LED with a FOV of 160° (cf. Fig. 13), and (ii) a 3W PinYuanLighting LED with a FOV of 60°*

different illumination conditions. The route followed by the two nodes is denoted by the dash line in Fig. 18, marked as 'route'. When either node A or node B passes the central circle, they are not aligned and thus can affect the VLC link. We assume node B needs to transmit data continuously to node A. The payload of each frame sent by node B is 200 bytes. We place a lamp with a 11W LED of the brand 'daylight' at the end of the round about to act as a road light. We perform this experiment under two illumination conditions: with all lights in the office off, except for the 'street light' (to emulate night conditions) and with all lights on (we turn on both the 'street light' and office light to emulate daylight conditions, since sunlight is much stronger than office light). The results are shown in Fig. 19(a) and (b), respectively. *Each marker 'x' represents the reception of one frame*, and the time in the x-axis is normalized to capture the beginning and end of the route, since the time taken to cover the route at each run is

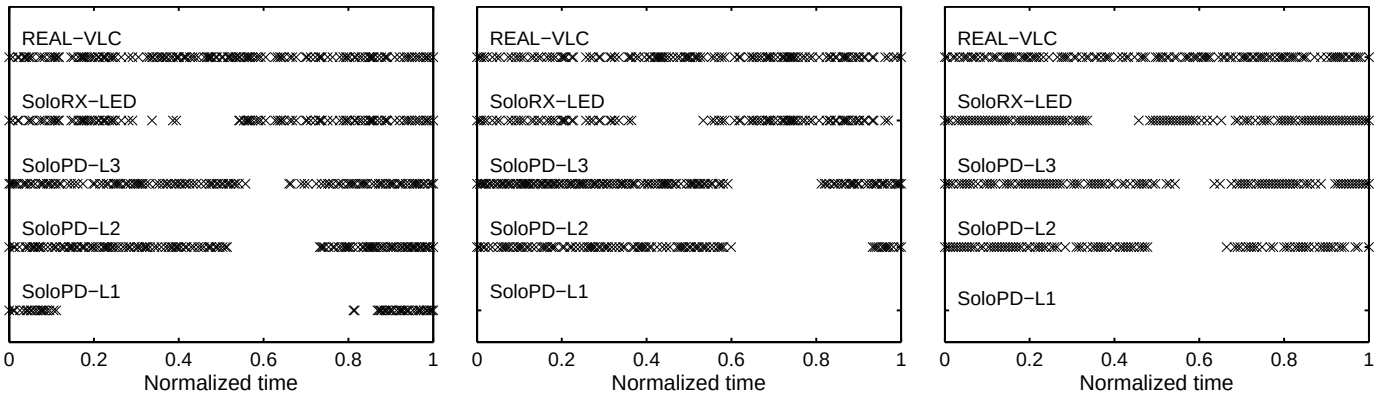

(a) All office lights are off, except the 'street light' (*emulate night). The White LED with a FOV of 160° is used at node B. Distance between the two nodes is 0.5 m*

(b) All office lights and the 'street light' are on (*emulate daylight). The White LED with a FOV of 160° is used at node B. Distance between the two nodes is 0.5 m*

(c) All office lights and the 'street light' are on (*emulate daylight). A 3W PinYuanLighting LED with a FOV of 60° is used at node B. Distance between the two nodes is 2.5 m*

Fig. 19. Performance evaluation in a scaled down smart car application. Each marker 'x' represents the reception of one frame *(payload is fixed to 200 bytes)*

not exactly the same. Horizontal white spaces between any two discontinuous markers 'x' imply that the communication link is lost for that amount of time.

In our evaluation, we consider different configurations of the receiver. First, we perform the experiments by setting different sensitivity levels at the PD (SoloPD-*X*). Then, we run the experiment using only the RX-LED (SoloRX-LED). Finally, we run the experiment with our visible light link, REAL-VLC.

The evaluation results are shown in Fig. 19. We can observe that at the highest sensitivity (SoloPD-L1), the PD has a poor performance at 'night' when the node is in the vicinity of the road lamp, and the link does not exist during the 'day', as shown in Fig. 19(b). As the PD's sensitivity is decreased (SoloPD-L2 and -L3), the link becomes more resilient. But we need to consider that indoor lighting, which was used in our experiment to resemble daylight, is not as strong as sunlight, c.f. Fig. 1. If the experiments were to be performed outdoors with daylight, links would disappear. The SoloRX-LED configuration performs reasonably well in both scenarios (day and night) except for the area close to the round where the line of alignment is affected.

On the other hand, our REAL-VLC provides constant connectivity across the board and decodes the highest number of packets.[8] *We can observe that it is the only configuration that maintains the link in darkness, under light and for straight and curve paths.* This benefit comes from the two main properties of our Data Link Layer: the ability to adjust the resistor of the PD based on ambient noise floor, and the parallel processing of streams received from the PD and RX-LED. Similar results can be observed in Fig. 19(c). There, the two nodes are kept at a distance of 2.5 m and a 3W LED with a FOV of 60° (the brand is 'PinYuanLighting') is used at node B.

VII. Discussion

In this work, we investigate a critical problem to bring VLC systems into reality: how to provide a reliable visible light link for low-end platforms. In this section, we expose the limitations of our current work and discuss potential research directions and enhancements.

A. Future enhancement of the implementation

So far, our implementation can only achieve a throughput of around 12 Kbp/s. The bottleneck of this low achievable throughput is due to the speed at which the symbols are sampled from the ADC by our driver (which is implemented in the Linux kernel). The Linux kernel fails to provide accurate timing once past a certain sampling speed. To solve this, adding an FPGA or micro-controller, or use the Programmable Real-time Unit (PRU) of the BBB to implement the PHY layer (especially the sampling) can help.

Other limitations of the implementation are the short range and narrow coverage of RX-LED. The short range is due to the fact that we only use LEDs up to 3W as transmitter and the transmission power is limited. This can be improved greatly by adopting common off-the-shelf brighter LEDs that have higher transmission power by default. To solve the narrow coverage of RX-LED, we plan to expand the reception coverage through an approach similar to the one that is adopted in [13] to enlarge the transmission coverage.

B. Methods for solving PD's saturation

The saturation of a PD can be changed through many ways [15]. While this work explored the impact of gain control in the transimpedance amplifier, other methods could also provide benefits, e.g., changing the reverse bias voltage applied to a PD. Dynamically changing the reverse bias voltage according to the ambient light noise and the aimed throughput is a tradeoff worth exploring in the future. In this work, we choose to explore the gain control to solve PD's saturation problem because it does not impact the transmission rate.

C. More types/numbers of photodetectors

In this work we only use two different types of photodetectors, a normal PD and a RX-LED. Our proposed REAL-VLC

[8]There are still some intermittent losses under our solution REAL-VLC. These losses are due to the computation overhead as we explain in Sec. VI-B.

is built upon the characteristics of these two photodetectors. To further improve the performance, we can scale the design in two dimensions: (1) use a number of different types of photodetectors. As presented in Fig. 3, different photodetectors have different tradeoffs between spectral response and FOV. Therefore, we can design a receiver with a number of different photodetectors to work under various ambient environments. For example, we can add a photodetector of the type "wide spectral response, wide FOV" to REAL-VLC to improve the communication range under static and "dark" environments. (2) use a number of certain type of photodetector. For example, we can use an array of "narrow spectral response, narrow FOV" photodetectors to maintain a reliable link under mobile scenarios with strong ambient light.

VIII. Related Work

Transforming any LED light into a wireless transmitter is already creating a new range of exciting applications that will form the basic infrastructure of the IoL: broadband communication, sensing, proximity interaction, localization, etc. These works can be categorized into four areas.

High-end indoors. Researchers have investigated VLC for next-generation networks with complex optical front-ends and/or sophisticated modulation methods [1], [16], [17], [18], [19]. Most of these efforts are based on resource-rich platforms, e.g. WARP [1], [20], and aim at increasing data rates in point-to-point scenarios under mild lighting conditions. While most of these studies are not relevant to ours, some are orthogonal and could be used to improve the performance of our receiver. For example, in [1], the transmitter adjusts the transmission rate upon detecting SNR changes at the receiver, in [19], multi-element transmitters are designed to improve the quality of signal distribution in a room, and in [18], PDs with different FOVs are used to increase the data rate. These studies could provide a dynamic adaption of the PHY rate which is currently fixed in our work.

High-end outdoors. There are few VLC studies that venture outdoors. Vehicle-to-vehicle communication is an exemplary application [21], [22]. They rely mainly on simulations, but some evaluate VLC prototypes outdoors with sunlight. From these studies we learned the importance of adjusting the FOV to avoid saturation due to sunlight, particularly in [21]. The prototypes however rely on very expensive optical front-ends such as Thorlabs-PDA100A [22], whose cost is upwards of 300 USD. Our optical front-end is designed to operate in tiny transceivers for IoL and it costs less than 10 USD[9].

Low-end indoors. Recently, a range of exciting applications have been developed with low-end VLC platforms: sensing human motions [23], interaction [24], and indoor localization [25], [26]. These low-end platforms sit at the opposite extreme of high-end (Mb/s-Gb/s) VLC systems: they trade throughput (Kb/s) for cost and simplicity. Our system is also low-end and borrows the general idea of leveraging LEDs as receivers from [5], [27]. But it differs from these previous work on two facts: i) we do not rely on a single photodetector; and ii) we do not focus solely on the simpler case of indoor scenarios with static lights. Our system provides a more flexible and reliable link to tackle challenges related to dynamic ambient light and mobility.

Low-end outdoors. Low-end outdoors VLC has received little attention so far. In our previous position paper [28], we *initially* exploited the advantages of LED acting as a receiver for outdoor scenarios with sunlight, and *simply* combined it with the traditional solution using PDs as a receiver. In this paper, we largely extends that study in three main ways: *(1)* We provide the tradeoff analysis regarding the spectral response, sensitivity and communication range of using the PD and RX-LED as receivers. *(2)* We harness adaptive parameters at the PHY (gain control and decoding threshold) and Data Link Layers (additive and parallel decoding comparison) to improve the system performance in a variety of ambient lighting conditions. *(3)* We evaluate our solution under various scenarios with different dynamics in mobility and ambient light intensity, and with a scaled down application.

[9]As described before, we design two receiving chains to achieve a reliable and adaptive receiver. For the additional chain, the cost is only around 2 USD.

IX. Conclusion

Motivated by the vision of the Internet of Lights (IoL), we investigated the challenges associated with visible light links. We identified the limitations and tradeoffs of two optical receivers, PDs and LEDs (working as receivers), and showed that they have complementary properties. Based on this insight, we designed and implemented a new cost-efficient Data Link Layer that is resilient to dynamics caused by changes in illumination and directionality. We evaluated our system under different dynamics, and the results show that our solution outperforms methods relying solely on either a PD or an LED. The proposed receiver is designed to operate in tiny transceivers for the IoL and only costs a few USD. It has been integrated in the OpenVLC platform (www.openvlc.org) and will be made available for the research community to investigate new networking challenges arising from the IoL and for the reproducibility of our findings.

References

[1] J. Zhang, X. Zhang, and G. Wu, "Dancing with light: Predictive in-frame rate selection," in *IEEE INFOCOM*, 2015, pp. 1–9.

[2] C. Rumelhard, C. Algani, and A.-L. Billabert, *Microwaves Photonic Links: Components and Circuits*. John Wiley & Sons, 2013.

[3] P. Pathak, X. Feng, P. Hu, and P. Mohapatra, "Visible light communication, networking, and sensing: A survey, potential and challenges," *IEEE Communications Surveys & Tutorials*, 2015.

[4] P. Dietz, W. Yerazunis, and D. Leigh, "Very low-cost sensing and communication using bidirectional LEDs," in *TR2003-35*, 2003.

[5] S. Schmid, G. Corbellini, S. Mangold, and T. R. Gross, "LED-to-LED visible light communication networks," in *ACM MobiHoc*, 2013.

[6] T. Li, Q. Liu, and X. Zhou, "Practical human sensing in the light," in *MobiSys*, 2016, pp. 71–84.

[7] Q. Lin, A. Armin, P. L. Burn, and P. Meredith, "Filterless narrowband visible photodetectors," *Nature Photonics*, 2015.

[8] Y. Acharya, "Spectral and emission characteristics of LED and its application to LED-based sun-photometry," *Optics & Laser Technology*, vol. 37, no. 7, pp. 547–550, 2005.

[9] S. Li and A. Pandharipande, "Led-based color sensing and control," *IEEE Sensors Journal*, vol. 15, no. 11, pp. 6116–6124, Nov 2015.

[10] J. M. Kahn and J. R. Barry, "Wireless infrared communications," *Proceedings of the IEEE*, vol. 85, no. 2, pp. 265–298, 1997.

[11] P. E. Gray and C. L. Searle, *Electronic principles: Physics, models, and circuits*. Wiley, 1969.

[12] Q. Wang, D. Giustiniano, and D. Puccinelli, "OpenVLC: Software-Defined Visible Light Embedded Networks," in *VLCS*, 2014, pp. 1–6.

[13] L. Klaver and M. Zuniga, "Shine: A Step Towards Distributed Multi-Hop Visible Light Communication," in *IEEE MASS*, 2015, pp. 1–9.

[14] R. Matzner and F. Englberger, "An snr estimation algorithm using fourth-order moments," in *IEEE International Symposium on Information Theory*, Jun 1994.

[15] "Thorlabs: Photodiode Saturation and Noise Floor," *https://goo.gl/vjWpwL*.

[16] D. Tsonev, S. Videv, and H. Haas, "Light fidelity (Li-Fi): towards all-optical networking," in *SPIE*, vol. 9007, 2013, pp. 900 702–900 702–10.

[17] S. Wu, H. Wang, and C.-H. Youn, "Visible light communications for 5G wireless networking systems: from fixed to mobile communications," *IEEE Network*, vol. 28, no. 6, pp. 41–45, Nov 2014.

[18] C. He, T. Q. Wang, and J. Armstrong, "Performance of optical receivers using photodetectors with different fields of view in a mimo aco-ofdm system," *Journal of Lightwave Technology*, pp. 4957–4967, 2015.

[19] Y. Eroglu, A. Sahin, I. Guvenc, N. Pala, and M. Yuksel, "Multi-element transmitter design and performance evaluation for visible light communication," in *IEEE Globecom Workshops*, 2015, pp. 1–6.

[20] M. Rahaim, A. Miravakili, T. Borogovac, T. Little, and V. Joyner, "Demonstration of a software defined visible light communication system," in *Mobicom*, 2011.

[21] C. B. Liu, B. Sadeghi, and E. W. Knightly, "Enabling vehicular visible light communication (V2LC) networks," in *VANET*, 2011, pp. 41–50.

[22] S.-H. Yu, O. Shih, H.-M. Tsai, and R. Roberts, "Smart automotive lighting for vehicle safety," *IEEE Communications Magazine*, vol. 51, no. 12, pp. 50–59, 2013.

[23] T. Li, C. An, Z. Tian, A. T. Campbell, and X. Zhou, "Human sensing using visible light communication," in *ACM MobiCom*, 2015.

[24] C. Zhang, J. Tabor, J. Zhang, and X. Zhang, "Extending mobile interaction through near-field visible light sensing," in *MobiCom*, 2015.

[25] L. Li, P. Hu, C. Peng, G. Shen, and F. Zhao, "Epsilon: A visible light based positioning system," in *NSDI*, April 2014, pp. 331–343.

[26] Y.-S. Kuo, P. Pannuto, K.-J. Hsiao, and P. Dutta, "Luxapose: Indoor positioning with mobile phones and visible light," in *ACM MobiCom*, 2014, pp. 447–458.

[27] D. Giustiniano, N. Tippenhauer, and S. Mangold, "Low-complexity visible light networking with LED-to-LED communication," in *IFIP Wireless Days*, 2012, pp. 1–8.

[28] Q. Wang, D. Giustiniano, and O. Gnawali, "Low-cost, flexible and open platform for visible light communication networks," in *ACM Workshop on Hot Topics in Wireless*, 2015.

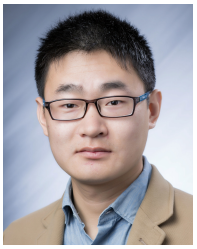

Qing Wang (S'13–M'17) is currently Postdoc Associate with KU Leuven, Belgium. He received his Ph.D. and M.S. degrees from the University Carlos III of Madrid and IMDEA Networks Institute in 2016 and 2012, respectively. Prior to that, He received his B.E. and M.S. degrees from the University of Electronic Science and Technology of China, in 2008 and 2011, respectively. His research interests include visible light communication, Internet of things and device-to-device communication.

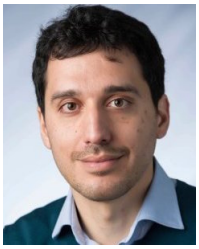

Domenico Giustiniano (S'06–M'13–SM'17) is Research Associate Professor at IMDEA Networks Institute and leader of the Pervasive Wireless Systems Group. He was formerly a Senior Researcher and Lecturer at ETH Zurich and a Post-Doctoral Researcher at Disney Research Zurich and at Telefonica Research Barcelona. He was awarded a Ph.D. from the University of Rome Tor Vergata in 2008. He devotes most of his current research to emerging areas, including visible light communication, mobile indoor localization, and collaborative spectrum sensing. He is an author of more than 60 international papers and an inventor of five patents.

Marco Zuniga (M'14) is Assistant Professor at the Department of Computer Science at Delft University of Technology, the Netherlands. Before this appointment, he was a member of the research staff at Xerox Research Labs; an IRCSET fellow at the National University of Ireland, Galway; and a senior researcher at the University of Duisburg-Essen, Germany. He obtained his PhD and MSc in Electrical Engineering from the University of Southern California and his BSc in Electronics Engineering from the Pontificia Universidad Catolica del Peru. His research interests are on the areas of cyber-physical systems and mobile computing.